An Evolving Understanding of Enigmatic Large Ripples on Mars

Mathieu G. A. Lapôtre[1], Ryan C. Ewing[2], and Michael P. Lamb[3]

[1]Department of Geological Sciences, Stanford University, Stanford, CA, USA.

[2]Department of Geology & Geophysics, Texas A&M, College Station, TX, USA.

[3]Division of Geological & Planetary Sciences, California Institute of Technology, Pasadena, CA, USA.

Corresponding author: Mathieu G. A. Lapôtre (mlapôtre@stanford.edu)

Key Points:

- A new model predicts small windblown ripples should grow to be meter-scale on Mars.
- That model cannot explain some observations that appear to be more consistent with an aerodynamic origin for large martian ripples.
- Answering remaining questions on large-ripple formation will require new observations, both in situ and from wind-tunnel experiments.

This article has been accepted for publication and undergone full peer review but has not been through the copyediting, typesetting, pagination and proofreading process, which may lead to differences between this version and the Version of Record. Please cite this article as doi: 10.1029/2020JE006729.

Abstract

Two scales of ripples form in fine sand on Mars. The larger ripples were proposed to have an equilibrium size set by an aerodynamic process, making them larger under thinner atmospheres and distinct from smaller impact ripples. Sullivan et al. (2020) show that large ripples can develop in a numerical model due to Mars' low atmospheric pressure. Although their proposed growth-limiting mechanism is consistent with an aerodynamic process, they argue that the ripples in their model are simply large versions of impact ripples, not a separate class of ripples. Here, we explore this debate by synthesizing recent advances in large-ripple formation. Although significant knowledge gaps remain, it is clear that large martian ripples are larger under thinner atmospheres, and thus remain a powerful paleoclimate indicator.

Plain Language Summary

Earth's sandy deserts host small ripples and large dunes, but Mars' dune fields also host a third type of sedimentary pattern – large ripples with meter-scale spacings. The large ripples were previously proposed to be distinct from small Earth-like ripples on Mars, and their size was suggested to result from the low atmospheric pressure on Mars. In contrast, Sullivan et al. (2020) show that, in a numerical model, small ripples can grow large on Mars. Here, we explore this debate by synthesizing recent advances in large-ripple formation. While significant knowledge gaps remain, it is clear that large martian ripples are larger under thinner atmospheres, and thus remain a powerful tool to probe Mars' ancient climate.

In December 2015, the Curiosity rover made tantalizing observations of windblown bedforms as it arrived near the first dune field ever visted on another planet (Fig. 1a; Bridges and Ehlmann, 2017; Lapôtre and Rampe, 2018). In particular, puzzling ripples with consistent meter-scale wavelengths, found both on top of dunes and outside of the dune field in isolated ripple fields (Fig. 1a), caught the attention of scientists and space enthusiasts alike. These large martian ripples are far larger than the more familiar decimeter-wavelength wind ripples found on Earth. Such large ripples were known to be widespread on Mars from orbital imagery (Bridges et al., 2012a) and some had even been seen with the Mars Exploration Rovers (e.g., Greeley et al., 2004; Sullivan et al., 2005; 2008). However, Curiosity's observations were unique; this was the first time that large ripples were seen to form concurrently with small, decimeter-scale ripples, which are too small to be seen from orbit, and large sand dunes.

Three coexisting scales of bedforms challenged existing models for ripple formation, which were developed to match observations on Earth of a single scale of small ripples forming on larger sand dunes. Prior to Curiosity's observations, the large martian ripples were thought to be equivalent to small terrestrial *impact ripples* – formed by a particle impact-driven instability – but were larger on Mars because sand grains experience longer saltation trajectories as a result of the lower gravitational acceleration and thin atmosphere (e.g., Almeida et al., 2008; Durán Vinent et al., 2014). However, Curiosity revealed that the large ripples are not simply larger versions of the small ripples; they in fact coexist with the small ripples.

Lapôtre et al. (2016), Ewing et al. (2017), and Baker et al. (2018a) established that small and large ripples were active simultaneously, as shown by the absence of reworking of their respective crest lines and direct observations of the timing of their migration (from the ground and from orbit). On Earth, large ripples can form in poorly sorted sand (called *coarse-grained ripples*,

megaripples, or sometimes *granule ripples*; these terms are used here without implications for the transport modes of different grain-size fractions) where a coarser grain population armors the crest of large ripples (e.g., Figs. 3 and 7 of Sullivan et al. (2020) and Fig. 1 of Lorenz (2020)). The martian ripples, however, were found in well sorted fine sand (e.g., Lapôtre et al., 2016; Ehlmann et al., 2017; Ewing et al., 2017; Sullivan and Kok, 2017; Weitz et al., 2018). Lapôtre et al. (2016) and Ewing et al. (2017) showed that both large ripples and small ripples in well sorted sand had relatively uniform and distinct size distributions and lacked bedforms in the ~20–80 cm range, suggesting that the two scales of ripples had different equilibrium sizes. They postulated that the two scales of ripples require different mechanisms to set the distinct ripple sizes.

Some large martian ripples have sinuous crests and highly asymmetric profiles with grainfall and grainflow (avalanche)-dominated slip faces, and exert a strong topographic control on the local wind field as evidenced by deflection of small ripples (Fig. 1b; Lapôtre et al., 2016). Because these characteristics are more similar to current ripples formed in flowing water, as compared to ballistically-formed impact ripples, Lapôtre et al. (2016) hypothesized that the equilibrium size of large martian ripples may be controlled by an aerodynamic mechanism, where wind drag at the ripple crest is important in limiting its size, and they used the term *wind-drag ripples*.

Since the work of Lorenz et al. (2014) who compiled the wavelength of ripples spanning 23 km of elevation range in the Tharsis region, it was known that the wavelength of large ripples on Mars is larger with decreasing atmospheric pressure. In addition to the Lorenz et al. (2014) dataset, Lapôtre et al. (2016) compiled the wavelength of large martian ripples globally, where they are found in association with dark-sand dunes. They showed that the wavelength of large martian ripples, λ, follows roughly the same relationship with atmospheric density as what is expected of current ripples forming under water on Earth (Fig. 2) – that is that $\lambda^* = \frac{\lambda u_*}{\nu}$ (u_* the wind shear

velocity, ν the kinematic viscosity of the atmosphere) is proportional to $\chi^{1/3}$, where $\chi = \mathrm{Re}_p\sqrt{\tau_*}$ with Re_p the particle Reynolds number and τ_* the Shields number. Lapôtre et al. (2017a) further noted that χ, which they called the Yalin number, is also proportional to a Reynolds number, $\frac{l_{\mathrm{sat}}u_*}{\nu}$, where the length scale, $l_{\mathrm{sat}} \propto \sqrt{\frac{u_*^2 d}{Rg}}$, is a proposed typical saturation length scale for bedload transport (e.g., Charru et al. 2013; also similar to Durán Vinent et al., 2019), with d the grain diameter, g the acceleration of gravity, and $R = \frac{(\rho_s - \rho)}{\rho}$ the specific submerged density of sediment (where ρ_s and ρ are the sediment and fluid densities, respectively).

Lapôtre et al. (2016) used the term wind drag generically to hypothesize that drag from the wind plays an important role in limiting the size of large martian ripples; they did not detail the exact mechanism. This terminology has led to confusion in Sullivan et al. (2020) because Bagnold (1941) also used the term wind-drag ripples, but his intention was to describe ripples that formed by sediment transport that was primarly driven by wind drag, rather than particle impacts (see also Wilson, 1972; Yizhaq et al., 2020). However, because of the low atmospheric pressure on Mars, there is little doubt that saltation-driven impacts control the continuation, and perhaps even the onset (Sullivan et al., 2017), of sediment transport on Mars – not wind drag (Sullivan and Kok, 2017). This apparent contradiction led Sullivan et al. (2020) to conclude that ripple sizes cannot be controlled by wind drag, because sediment transport on Mars is controlled by particle-impact driven processes. However, despite the perhaps unfortunate commonality of descriptors – impact and wind drag – the processes that determine sediment initial motion can be independent of the processes that determine ripple size (Lapôtre et al., 2018). Indeed, Lapôtre et al. (2016) used the impact threshold velocity (Kok, 2010) in their scaling relationship for ripple size; they did not use the fluid threshold. Regardless of whether initial sediment motion occurs by wind drag or impact

processes, the explanation for Curiosity's observation of two scales of coexisting ripples remains a matter of debate.

To address this controversy, Sullivan et al. (2020) combined sediment mass balance with inputs from a particle saltation model (Kok and Renno, 2009) to simulate the time evolution of an initially-flat bed seeded with small topographic defects to trigger ripple formation. They did not implement a growth-limiting mechanism in their model, such that modeled ripples grew indefinitely, which precluded a comparison to the wavelengths of ripples observed on Mars and to the scaling analysis of Lapôtre et al. (2016). To demonstrate that the model is able to reproduce the coexistence of multiple scales of ripples, Sullivan et al. (2020) seeded their ripple profile a second time with small topographic defects once large ripples had already evolved; the defects developed a second generation of small ripples that piggy-backed onto the now larger first-generation ripples. Because, under their model, large ripples can readily grow from small impact-generated ripples, Sullivan et al. (2020) argued that large martian ripples are the same as the small impact ripples, they just had more time to grow. However, while the model can produce two scales of growing ripples, the ripples did not reach an equilibirium size. Rather, their relative scales were determined precisely by the imposed timing of seeding the profile with defects. For example, for a continuous defect-seeding of the evolving profile, as would be the case in nature, one might expect the model to produce a full continuum of ripple sizes. Their results are in contrast to rover and orbiter observations on Mars that show that both the small and large ripples stay approximately the same size as they migrate (e.g., Ewing et al., 2017; Vaz et al., 2017; Fig. 1b). Thus, the question of why Mars hosts two distinct coexisting scales of ripples remains unanswered.

Instead of implicating separate mechanisms that set the size of the small and large ripples, Sullivan et al. (2020) speculate, but did not model, that two scales would inherently arise because

fetch is insufficient for small ripples to grow between two consecutive large-ripple crests. This hypothesis remains untested. Given the observed wavelengths and migration rate of small (e.g., Baker et al., 2018a) and large (e.g., Bridges et al., 2012b) ripples, it is at least geometrically possible that several ripples with > 40 cm wavelengths could fit between two consecutive large-ripple crests; but these intermediate ripples have not been observed in fine sand on Mars (Lapôtre et al., 2016; Ewing et al., 2017). Such "gap" ripples can exist, as shown by Sullivan et al. (2020) and Lorenz (2020), but only where there is a population of coarser grains concentrating at ripple crests. Although there likely is a continuum of processes that genetically relate the large ripples found in fine dune sand and those with coarse-grained crests found in ripple fields (Fig. 1a; Lapôtre et al., 2018), small and large ripples were both formed in fine sand within the dune field observed by Curiosity, and a coarse-grained cap did not exist (e.g., Ewing et al., 2017; Weitz et al., 2018).

Sullivan et al. (2020) note that color differences between the crests and bulk of coarse-grained ripples, found in ripple fields outside of the dune field in Gale crater (Fig. 1a), correlate with measured grain size (e.g., Fig. 1c), and argue that this correlation indicates that a coarser population must also exist at the crests of ripples migrating onto the dunes (Fig. 1b), where subtle color differences can also be seen from highly stretched Mastcam images. Sullivan et al. (2020) discard a direct measurement of fine sand that had been performed over a large-ripple crest on top of a dune because it was made near the lateral tip of a large-ripple crest near the crests of small ripples (Fig. A3D in Sullivan et al., 2020), and may thus have been more representative of the small ripple crests than of the large ripple itself. However, many more grain-size measurements have now been performed and reported (Weitz et al., 2018), corroborating that dune sand is relatively well sorted and finer than medium sand at large ripple crests (e.g., Kibnas, Flume Ridge, Waweig, Ripogenus, Avery Peak targets; Weitz et al., 2018). The coarser fraction mantling the crests of large ripples in

ripple fields (as shown by Sullivan et al., 2020) was also observed to concentrate at the upwind edge of the dune field (e.g., Barby target; Weitz et al., 2018), consistent with lags commonly observed at the edge of terrestrial dune fields (Ewing et al., 2017), where coarser grains cannot move up-stoss due to the effect of adverse slopes on sand flux (e.g., Tsoar et al., 1996; Iversen and Rasmussen, 1999). Migrating "megaripples," interpreted as coarse-grained ripples by Silvestro et al. (2020), stop migrating when approaching the stoss slope of active dunes, confirming that coarser fractions cannot be transported up-stoss into dune fields.

It seems more likely that the subtle color differences between ripple crests and bulk sand on top of dunes, reflect compositional differences rather than sharp grain-size contrasts as are observed in ripple fields (Fig. 1c). All compositional measurements performed over windblown sands to date, including within the dune field investigated by Curiosity, revealed mineral sorting (e.g., Achilles et al., 2017; Cousin et al., 2017; Ehlmann et al., 2017; Johnson et al., 2017; 2018; Lapôtre et al., 2017b; O'Connell-Cooper et al., 2017; 2018; Rampe et al., 2018), with large-ripple crests being enriched in mafic phases (explaining their bluer hue). A good question then is whether compositional sorting over dunes – with denser mafic grains concentrating at ripple crests – could have an equivalent effect to coarse grains in ripple fields. It seems unlikely; for a given grain size and given typical basaltic mineral densities, mafic grains could only weigh ~1.15 times more than bulk sand, at most, whereas for a given composition, 350 μm grains are ~12.7 times heavier than 150 μm grains.

In contrast with the model of Sullivan et al. (2020), Durán Vinent et al. (2019) proposed two aerodynamic mechanisms to explain both the initiation and equilibrium size of large martian ripples. Under their model, the minimum wavelength of ripples is dictated by the condition that any spatial shift between the locations of maximum bed stress and the ripple crest must exceed the

saturation length. The largest achievable wavelength, in turn, would be dictated by an aerodynamic response in the inner boundary layer (e.g., Abrams and Hanratty, 1985; Frederick and Hanratty, 1988; Charru et al., 2013) that shifts the location of maximum bed shear stress from upwind to downwind of the ripple crest. Importantly, only the scaling relationship of Lapôtre et al. (2016) and model of Durán Vinent et al. (2019) can quantatively explain the equilibrium wavelength of large ripples. Moreover, these theories also can explain the absence of large ripples on Earth in fine sand, as putative drag ripples are expected to be of similar size as terrestrial impact ripples under terrestrial atmospheric pressure (Fig. 2).

Although their model did not create equilibrium ripples, Sullivan et al. (2020) speculated that wind drag may play a role in limiting ripple growth. Bagnold (1941) hypothesized that impact ripples on Earth grow in size until they become just tall enough to intersect wind speeds capable of entraining grains past ripple crests through longer transport trajectories, preventing any further growth. Manukyan and Prigozhin (2009) also recognized that an increased probability of entrainment of the grains at the crest may contribute to the saturation of ripple growth, and successfully modeled the evolution of equilibrium impact ripples. Building on these hypotheses, Sullivan et al. (2020) argued that, owing to the thinner atmosphere on Mars, dynamic wind pressure at the crests of smaller ripples is low, allowing for grains to accumulate there. Intuitively, this growth-limiting mechanism might lead to equilibrium ripple heights that covary with atmospheric density – as is observed in the data and is predicted by the scaling relationship of Lapôtre et al. (2016).

Lapôtre et al. (2017a) noted that the Lapôtre et al. (2016) formulation of χ is well suited for bedload transport (i.e., where grain motion is dominated by rolling, sliding, and short non-ballistic hopping – most similar to the *creep* population in the eolian literature), as might be appropriate in

some places on Mars where eolian transport is thought to be of relatively low-energy (Baker et al., 2018a,b; Lapôtre et al., 2018; Sullivan and Kok, 2017). Like Lapôtre et al. (2016), Durán Vinent et al. (2019) also mathematically related the stability of large martian ripples to χ but using a formulation of the saturation length that scales with the average hop length of saltation trajectories ($l_{\mathrm{sat}} = \frac{\rho_{\mathrm{s}} u_t^2}{g(\rho_{\mathrm{s}} - \rho)}$, where u_t is the impact threshold shear velocity). Using l_{sat} for saltation from Durán Vinent et al. (2019) in the scaling relationship of Lapôtre et al. (2016) reveals a good fit to the data (Fig. 2; $\lambda^* \approx 600 \left(\frac{l_{\mathrm{sat}} u_*}{\nu}\right)^{1/3}$ for the global compilation of large ripples in dark sand). When using l_{sat} for saltation, large ripple wavelength is predicted to scale with $\left(\frac{u_t}{u_*}\right)^{2/3}$, such that $\lambda \sim (2.6 - 4.1)\left(\frac{u_t}{u_*}\right)^{2/3}$ for typical values of atmospheric density at rover landing sites (~0.01–0.02 kg/m^3). The effect of shear velocity on ripple size is thus negligible when wind speeds are close to the impact threshold, as is thought to be largely the case on Mars (e.g., Sullivan and Kok, 2017). Importantly, this formulation of saturation length is quantitatively consistent with observations and reconciles the discrepancies noted by Sullivan et al. (2020) between likely wind speeds and reconstructed u_* from bedform wavelengths.

As shown in Lapôtre et al. (2016; Fig. S10) and also noted by Sullivan et al. (2020) and Lorenz (2020), the Lapôtre et al. (2016) scaling relationship more robustly fits data collected by Lorenz et al. (2014) from Tharsis than data collected by Lapôtre et al. (2016) from dark-sand dunes globally (Fig. 2). Tharsis ripples appear different than ripples observed over dark-sand dunes, appearing overall less sharp and of higher albedo. Weaker winds on Tharsis, for example, could promote near-bed transport and the accumulation of dust between transport events, whereas more active ripples found in dune fields would be dominated by saltation. Differences could also result

from measurement bias; Lorenz et al. (2014) reported a mean wavelength of 0.5 m at their lowermost measurement elevation; however, the corresponding HiRISE image has a ground sample distance of 28.3 cm/pix (projected pixel scale of 25 cm/pix; HiRISE repository, https://hirise.lpl.arizona.edu/ESP_011928_2025) such that resolving objects less than ~85 cm across is challenging. In a cursory reinspection of the image, we found few linear features less than 3 pixel across and noted an abundance of ripples with wavelengths >~90 cm. For the sake of argument, we note that changing this single data point to 90 cm (Fig. 2) would strengthen the comparison of the Lapôtre et al. (2016) scaling relation, using the saturation-length formulation of Durán Vinent et al. (2019), to the data of Lorenz et al. (2014). The mechanistic relation is indistinguishable from the $\lambda \propto 1/\rho$ correlation proposed by Lorenz et al. (2014) and Lorenz (2020) under Mars-like pressures.

Despite some disagreements outlined here, the community is converging towards an aerodynamic control on the equilibrium wavelength of large ripples (Lapôtre et al., 2016), whether ripple size is limited by longer grain trajectories at ripple crests (Sullivan et al., 2020) or a shift in the boundary layer dynamics (Durán Vinent et al., 2019). However, the mechanics that allow two scales of ripples to form simultaneously in fine sand remain unclear. If the large ripples are impact ripples with an aerodynamically controlled equilibrium size, as proposed by Sullivan et al. (2020), it is then unclear what mechanism prevents intermediate ripples to form in well sorted sand. A single ripple growth-limiting mechanism cannot simultaneously explain two distinct equilibrium ripple sizes in monodisperse sand. The model of Durán Vinent et al. (2019) offers a new aerodynamic mechanism to explain the equilibrium wavelength of large ripples that does not rely on coarse grains, and is consistent with the observations and scaling analysis of Lapôtre et al. (2016), but they did not address the equilibrium size of small ripples mechanistically. If the large

ripple sizes are limited by the aerodynamic mechanism of Durán Vinent et al. (2019), then perhaps the small ripples are simply impact ripples as envisioned by Sullivan et al. (2020), but are limited to a similar scale as terrestrial wind ripples despite the lower atmospheric pressure on Mars. This idea is consistent with low-pressure wind tunnel experiments performed by Miller et al. (1987) that showed that a population of small ripples had a stable size under a wide range of atmospheric pressures, without significant changes in wavelength, whereas a second population of ripples grew in size with decreasing atmospheric pressure. Similarly, recent low-pressure wind-tunnel experiments also have demonstrated the characteristic wavelength of small impact ripples do not change substantially as atmospheric pressure is changed from terrestrial to martian values (Claudin et al., 2020).

In addition to numerical modeling, further progress towards understanding the formation of large martian ripples will require more observations and measurements of grain characteristics, their modes of transport, and the wind shear velocities associated with ripple creation, either in situ with landed spacecraft operating in an active dune field or through low-pressure wind-tunnel experiments on Earth. Such a mechanistic approach will be required to fully understand the mystery of large martian ripples (and possibly, of other bedforms under low-density atmospheres; e.g., Jia et al., 2017). However, it is clear that some ripples forming in well sorted sand under a thin martian atmosphere are larger than ripples found under a thicker terrestrial atmosphere (Lapôtre et al., 2016). Importantly, even on Mars today, ripples forming at higher elevation, where atmospheric density is lower, tend to have longer wavelengths than those forming at lower elevations, where atmospheric density is higher (Lorenz et al., 2014; Lapôtre et al., 2016). The latter statement is purely empirical and agnostic to formation process. As a result, and contrary to what was suggested by Lorenz (2020), the presence of sandstones formed by meter-scale

windblown ripples remains an important proxy for a thin paleoatmosphere, and an important tool to unravel when Mars lost its thicker atmosphere to become the cold and dry desert planet we know today.

Acknowledgments, Samples, and Data
This work was supported in part by NASA Grant 80NSSC20K0145 to M.G.A.L. No new data are presented in this manuscript.

References

Abrams, J., and Hanratty, T. J. (1985). Relaxation effects observed for turbulent flow over a wavy surface. *Journal of Fluid Mechanics*, 151, 443–455, https://doi.org/10.1017/S0022112085001045

Achilles, C., Downs, R. T., Ming, D. W., Rampe, E. B., Morris, R. V., Treiman, A. H., et al. (2017). Mineralogy of an active eolian sediment from the Namib Dune, Gale Crater, Mars. *Journal of Geophysical Research: Planets*, 122, 2344–2361, https://doi.org/10.1002/2017JE005262

Almeida, M. P., Parteli, E. J. R., Andrade Jr., J. S., and Hermann, H. A. (2008). Giant saltation on Mars. *Proceedings of the National Academy of Sciences of the United States of America*, 105(17), 6222–6226, https://doi.org/10.1073/pnas.0800202105

Baker, M., Lapôtre, M. G. A., Minitti, M. E., Newman, C. E., Sullivan, R., Weitz, C. M., Rubin, D. M., Vasavada, A. R., Bridges, N. T., and Lewis, K. W. (2018a). The Bagnold Dunes in southern summer: Active sediment transport on Mars observed by the Curiosity rover. *Geophysical Research Letters*, 45(17), 8853–8863, https://doi.org/10.1029/2018GL079040

Baker, M., Newman, C. E., Lapôtre, M. G. A., Sullivan, R., Bridges, N. T., and Lewis, K. W. (2018b). Coarse sediment transport in the modern martian environment. *Journal of Geophysical Research: Planets*, 123, 1380–1394, https://doi.org/10.1002/2017JE005513

Bagnold, R. (1941). *The Physics of Blown Sand and Desert Dunes* (Methuen and Co., London), Vol. 10

Bridges, N. T., Bourke, M. C., Geissler, P. E., Banks, M. E., Colon, C., Diniega, S., Golombek, M. P., Hansen, C. J., Mattson, S., McEwen, A. S., Mellon, M. T., Stantzos, N., and Thomson, B. J. (2012a). Planet-wise sand motion on Mars. *Geology*, 40(1), 31–34, https://doi.org/10.1130/G32373.1

Bridges, N. T., Ayoub, F., Avouac, J.-P., Leprince, S., Lucas, A., and Mattson, S. (2012b). Earth-like sand fluxes on Mars. *Nature*, 485, 339–342, https://doi.org/10.1038/nature11022

Bridges, N. T., and Ehlmann, B. L. (2017). The Mars Science Laboratory (MSL) Bagnold Dunes campaign, phase 1: Overview and introduction to the special issue. *Journal of Geophysical Research: Planets*, 123, 3–19, https://doi.org/10.1002/2017JE005401

Charru, F., Andreotti, B., and Claudin, P. (2013). Sand ripples and dunes. *Annual Review of Fluid Mechanics*, 45, 469–493, https://doi.org/10.1146/annurev-fluid-011212-140806

Claudin, P., Andreotti, B., Iversen, J. J., Merrison, J. P., and Rasmussen, K. R. (2020). Unexpected enhancement of saltation at Martian-like pressures. Abstract EP022-03 presented at 2020 Fall Meeting, AGU, San Francisco, CA, 1–17 Dec.

Cousin, A., Dehouck, E., Meslin, P. Y., Forni, O., Williams, A. J., Stein, N., et al. (2017). Geochemistry of the Bagnold dune field as observed by ChemCam and comparison with other aeolian deposits at Gale crater. *Journal of Geophysical Research: Planets*, 122, 2144–2162, https:// doi.org/10.1002/2017JE005261

Durán, O., Claudin, P., and Andreotti, B. (2014). Direct numerical simulations of aeolian sand ripples. *Proceedings of the National Academy of Sciences of the United States of America*, 111(44), 15665–15668, https://doi.org/10.1073/pnas.1413058111

Durán Vinent, O., Andreotti, B., Claudin, P., and Winter, C. (2019). A unified model of ripples and dunes in water and planetary environments. *Nature Geoscience*, 12, 345–350, https://doi.org/10.1038/s41561-019-0336-4

Ehlmann, B., Edgett, K., Sutter, B., Achilles, C., Litvak, M., Lapôtre, M., et al. (2017). Chemistry, mineralogy, and grain properties at Namib and High dunes, Bagnold dune field, Gale crater, Mars: A synthesis of Curiosity rover observations. *Journal of Geophysical Research: Planets*, 122, 2510–2543, https://doi.org/10.1002/2017JE005267

Ewing, R. C., Lapôtre, M. G. A., Lewis, K. W., Day, M., Stein, N., Rubin, D. M., Sullivan, R., Banham, S., Lamb, M. P., Bridges, N. T., Gupta, S., and Fischer, W. W. (2017). Sedimentary processes of the Bagnold Dunes: Implications for the eolian rock record of Mars. *Journal of Geophysical Research Planets*, 122(12), 2544–2573, https://doi.org/10.1002/2017JE005324

Frederick, K. A., and Hanratty, T. J. (1988). Velocity measurements for a turbulent nonseparated flow over solid waves. *Experiments in Fluids*, 6, 477–486, https://doi.org/10.1007/BF00196509

Greeley, R., Squyres, S., Arvidson, R., Bartlett, P., Bell, J., Blaney, D., et al. (2004). Wind related processes detected by the Spirit rover at Gusev Crater, Mars. *Science*, 305(5685), 810–813, https://doi.org/10.1126/science.1100108

Iversen, J.D., & Rasmussen, K.R. (1999). The effect of wind speed and bed slope on sand transport. *Sedimentology*, **46**, 723–731.

Jia, P., Andreotti, B., & Claudin, P. (2017). Giant ripples on copet 67P/Churyumov-Gerasimenko sculpted by sunset thermal wind. *Proceedings of the National Academy of Sciences of the United States of America*, **114**(10), 2509–2514, https://doi.org/10.1073/pnas.1612176114

Johnson, J., Achilles, C., Bell, J., Bender, S., Cloutis, E., Ehlmann, B., et al. (2017). Visible/near-infrared spectral diversity from in situ observations of the Bagnold Dune Field sands in Gale Crater, Mars. *Journal of Geophysical Research: Planets*, 122, 2655–2684, https://doi.org/10.1002/ 2016JE005187

Johnson, J. R., Bell, J. F. III, Bender, S., Cloutis, E., Ehlmann, B., Fraeman, A., et al. (2018). Bagnold Dunes campaign Phase 2: Visible/near-infrared reflectance spectroscopy of longitudinal ripple sands. *Geophysical Research Letters*, 45, https://doi.org/10.1029/2018GL079025

Kite, E. S. (2019). Geologic constraints on Early Mars climate. *Space Science Reviews*, 250(10), https://doi.org/10.1007/s11214-018-0575-5

Lapôtre, M. G. A., Ewing, R. C., Lamb, M. P., Fischer, W. W., Grotzinger, J. P., Rubin, D. M., Lewis, K. W., Ballard, M. J., Day, M., Gupta, S., Banham, S. G., Bridges, N. T., Des Marais, D. J., Fraeman, A. A., Grant, J. A., Herkenhoff, K. E., Ming, D. W., Mischna, M. A., Rice, M. S., Sumner, D. Y., Vasavada, A. R. and Yingst, R. A. (2016). Large wind ripples on Mars: A record of atmospheric evolution. *Science*, 353(6294), 55–58, https://doi.org/10.1126/science.aaf3206

Lapôtre, M. G. A., Lamb, M. P., and McElroy, B. (2017a). What sets the size of current ripples? *Geology*, 45(3), 243–246, https://doi.org/10.1130/G38598.1

Lapôtre, M. G. A., Ehlmann, B. L., Minson, S. E., Arvidson, R. E., Ayoub, F., Fraeman, A. A., Ewing, R. C., and Bridges, N. T. (2017b). Compositional variations in sands of the Bagnold Dunes, Gale crater, Mars, from visible-shortwave infrared spectroscopy and comparison with ground truth from the Curiosity rover. *Journal of Geophysical Research Planets*, 122(12), 2489–2509, https://doi.org/10.1002/2016JE005133

Lapôtre, M. G. A., Ewing, R. C., Weitz, C. M., Lewis, K. W., Lamb, M. P., Ehlmann, B. L., and Rubin, D. M. (2018). Morphologic diversity of martian ripples: Implications for large-ripple formation. *Geophysical Research Letters*, 45, 10229–10239, https://doi.org/10.1029/2018GL079029

Lapôtre, M. G. A., and Rampe, E. B. (2018). Curiosity's investigation of the Bagnold Dunes, Gale crater: Overview of the two-phase scientific campaign and introduction to the special collection. *Geophysical Research Letters*, 45(19), 10200–10210, https://doi.org/10.1029/2018GL079032

Lorenz, R. D., Bridges, N. T., Rosenthal, A. A., and Donkor, E. (2014). Elevation dependence of bedform wavelength on Tharsis Montes, Mars: Atmospheric density as a controlling parameter. *Icarus*, 230, 77–80, https://doi.org/10.1016/j.icarus.2013.10.026

Lorenz, R. D. (2020). Martian ripples making a splash. *Journal of Geophysical Research: Planets*, e2020JE006658, https://doi.org/10.1029/2020JE006658

Manukyan, E., and Prigozhin, L. (2009). Formation of aeolian ripples and sand sorting. *Physical Review E*, 79, 031303, hggpt://doi.org/10.1103/physreve.79.031303

Miller, J. S., Marshall, J. R., and Greeley, R. (1987). Wind ripples in low density atmospheres. *NASA Technical Memorandum*, 89810, 268–270.

O'Connell-Cooper, C., Spray, J., Thompson, L., Gellert, R., Berger, J., Boyd, N., et al. (2017). APXS-derived chemistry of the Bagnold dune sands: Comparisons with Gale crater soils and the global Martian average. *Journal of Geophysical Research: Planets*, 122, 2623–2643, https://doi. org/10.1002/2017JE005268

O'Connell-Cooper, C. D., Thompson, L. M., Spray, J. G., Berger, J. A., VanBommel, S. J., Gellert, R., et al. (2018). Chemical diversity of sands within the linear and barchan dunes of the Bagnold Dunes, Gale crater, as revealed by APXS onboard Curiosity. *Geophysical Research Letters*, 45, https://doi.org/10.1029/2018GL079026

Rampe, E. B., Lapôtre, M. G. A., Bristow, T. F., Arvidson, R. E., Morris, R. V., Achilles, C. N., et al. (2018). Sand mineralogy within the Bagnold Dunes, Gale crater, as observed in situ and from orbit. *Geophysical Research Letters*, 45(18), 9488–9497, https://doi.org/10.1029/2018GL079073

Silvestro, S., Chojnacki, M., Vaz, D. A., Cardinale, M., Yizhaq, H., and Esposito, F. (2020). Megaripple migration on Mars. Journal of Geophysical Research: Planets, 125(8), e2020JE006446, https://doi.org/10.1029/2020JE006446

Sullivan, R., Arvidson, R., Bell, J., Gellert, R., Golombek, M., Greeley, R., et al. (2008). Wind-driven particle mobility on Mars: Insights from Mars Exploration Rover observations at "El Dorado" and surroundings at Gusev Crater. *Journal of Geophysical Research*, 113, E06S07, https://doi. org/10.1029/2008JE003101

Sullivan, R., Banfield, D., Bell, J. F., Calvin, W., Fike, D., Golombek, M., et al. (2005). Aeolian processes at the Mars exploration rover Meridiani Planum landing site. *Nature*, 436(7047), 58–61, https://doi.org/10.1038/nature03641

Sullivan, R., and Kok, J. F. (2017). Aeolian saltation on Mars at low wind speeds. *Journal of Geophysical Research Planets*, 122(10), 2111–2143, https://doi.org/10.1002/2017JE005275

Sullivan, R., Kok, J. F., Katra, I., and Yizhaq, H. (2020). A broad continuum of aeolian impact ripple morphologies on Mars is enabled by low wind dynamic pressures. *Journal of Geophysical Research: Planets*, e2020JE006485, https://doi.org/10.1029/2020JE006485

Tsoar, H., White, B., & Berman, E. (1996). The effect of slopes on sand transport – numerical modelling. *Landscape & Urban Planning*, **34**, 171–181.

Vaz, D. A., Silvestro, S., Sarmento, P. T. K., and Cardinale, M. (2017). Migrating meter-scale bedforms on Martian dark dunes: Are terrestrial aeolian ripples good analogues? *Aeolian Research*, 26, 101–116, https://doi.org/10.1016/j.aeolia.2016.08.003

Weitz, C. M., Sullivan, R. J., Lapôtre, M. G. A., Rowland, S. K., Grant, J. A., Baker, M., and Yingst, R. A. (2018). Sand grain sizes and shapes in eolian bedforms at Gale crater, Mars. *Geophysical Research Letters*, 45(18), 9471–9479, https://doi.org/10.1029/2018GL078972

Wilson, I. G. (1972). Aeolian bedforms – their development and origins. *Sedimentology*, 19, 173–210, https://doi.org/10.1111/j.1365-3091.1972.tb00020.x

Yizhaq, H., Bel, G., Silvestro, S., Elperin, T., Kok, J. F., Cardinale, M., Provenzale, A., and Katra, I. (2019). The origin of the transverse instability of aeolian megaripples. *Earth and Planetary Science Letters*, 512, 59–70, https://doi.org/10.1016/j.epsl.2019.01.025

Yizhaq, H., Swet, N., Saban, L., and Katra, I. (2020). Rediscovery of the fluid drag ripples in wind tunnel experiments. *Sixth International Planetary Dunes Workshop*, Abstract 3005.

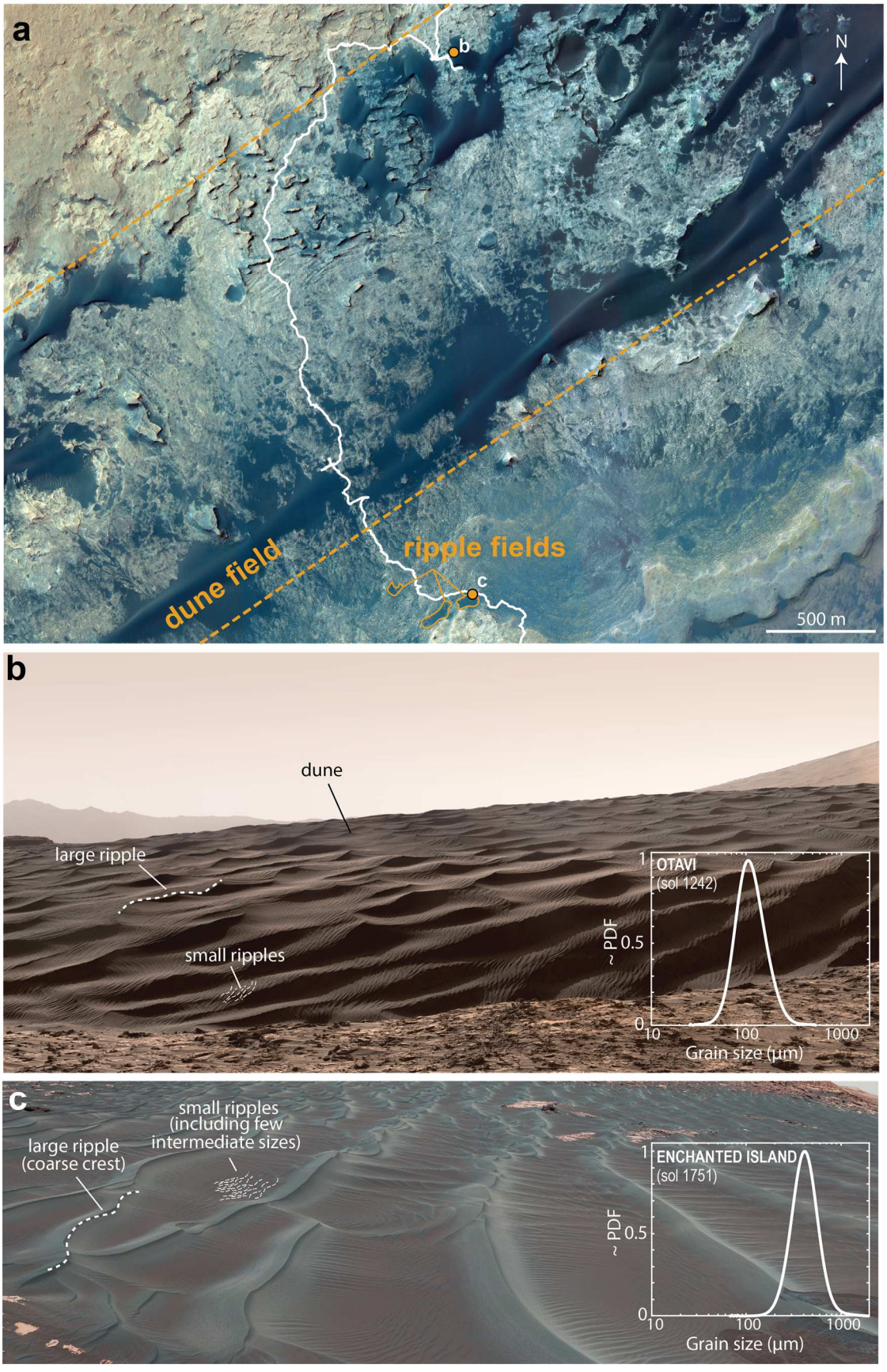

Figure 1. (a) HiRISE color mosaic showing Curiosity's traverse (white line) throughout the Bagnold Dune Field (bounded by dashed orange lines) and around ripple fields outside of the dune field (solid orange lines). Orange circles indicate the locations of panels b and c. (b) Mastcam mosaic of Namib Dune (sol 1192) on Mars, showing two distinct populations of ripples (Credit: NASA/JPL-Caltech/MSSS/Thomas Appéré). Inset: Kernel density of grain sizes measured at the Otavi target (sol 1242; Weitz et al., 2018). (c) Mastcam mosaic of transverse coarse-grained ripples at the Enchanted Island site (sol 1752) within a sand patch. Few coarse-grained ripples with wavelengths in the ~20- to 80-cm range are present near the image center (Lapôtre et al., 2018). There, color differences between crest and troughs is very clear, even without color stretching. Inset: Kernel density of grain sizes measured at the Enchanted Island target, a coarse-grained ripple crest (sol 1751; Weitz et al., 2018).

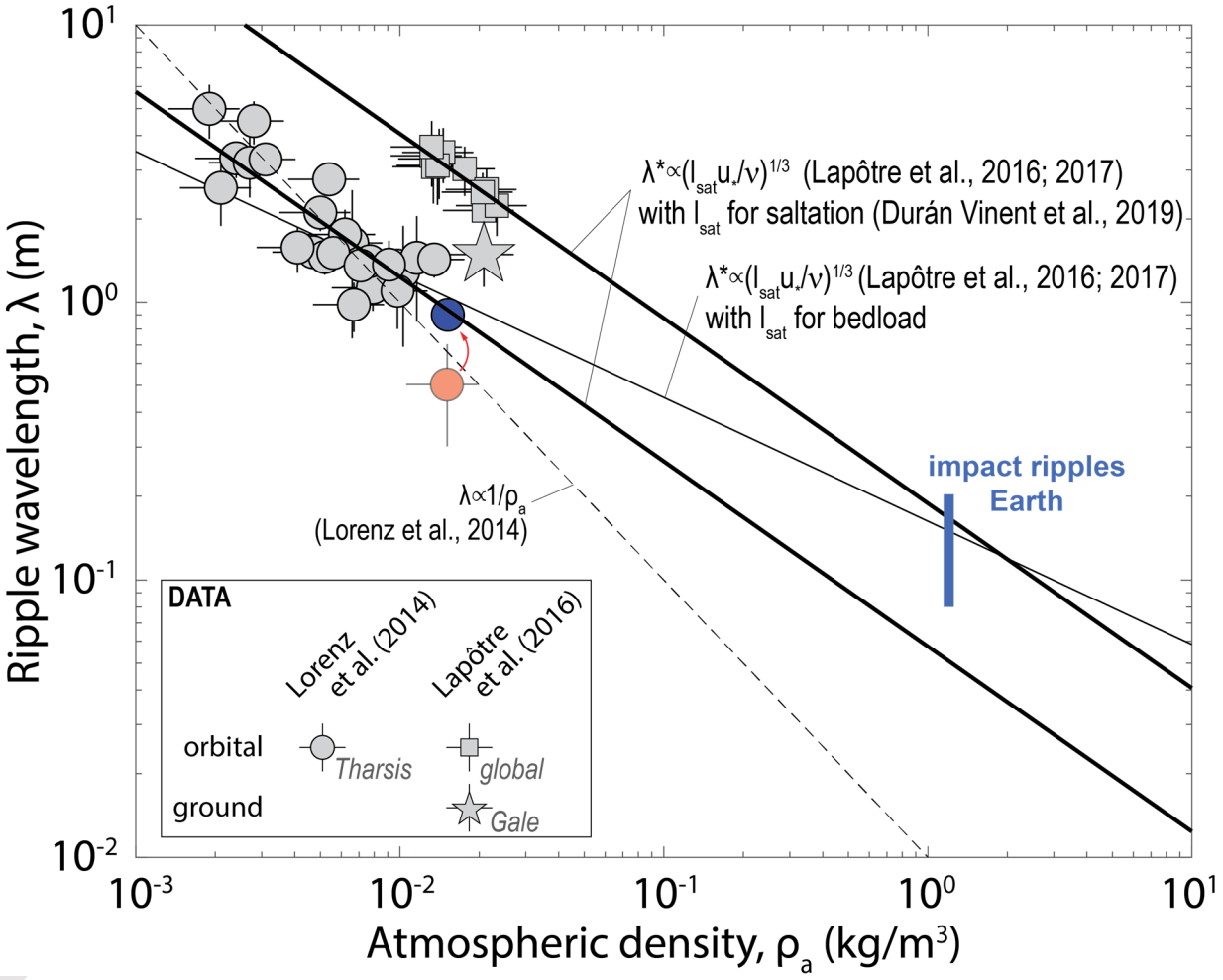

Figure 2. Wavelength of large martian ripples as a function of atmospheric density (adapted from Fig. S10 in Lapôtre et al., 2016). Red circle is a data point from Lorenz et al. (2014) indicating a mean ripple wavelength ~ 2 HiRISE pixels across; blue circle is our rough estimate of minimum ripple size upon inspection of the same image.